AD-A122 877 DEVELOPMENT OF PHOTOACOUSTIC SPECTROSCOPY FOR THE STUDY 1/1
OF BIOFILM FORMATION UNDER WATER(U) DELAWARE UNIV
NEWARK COLL OF MARINE STUDIES S C DEXTER SEP 82
UNCLASSIFIED N00014-77-C-0064 F/G 7/4 NL

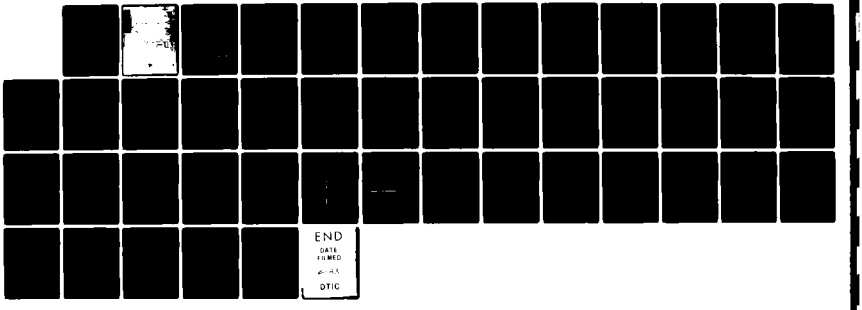

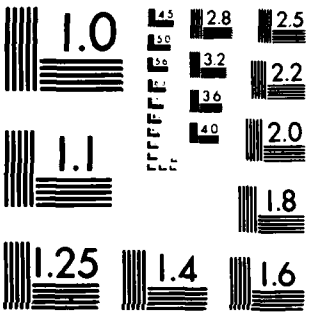

MICROCOPY RESOLUTION TEST CHART
NATIONAL BUREAU OF STANDARDS-1963-A

DEVELOPMENT OF PHOTOACOUSTIC SPECTROSCOPY FOR THE STUDY OF BIOFILM FORMATION UNDER WATER

FINAL REPORT

TO:

Office of Naval Research
Department of the Navy
Arlington, Virginia

CONTRACT:

N00014-77-C-0064

Through the Oceanic Biology Program
Ocean Science & Technology Detachment
NSTL Station, MS 39529

PRINCIPAL INVESTIGATOR:

Stephen C. Dexter
College of Marine Studies
University of Delaware
700 Pilottown Road
Lewes, DE 19958

September 1982

I. INTRODUCTION

A growing body of literature from a number of diverse scientific disciplines has documented that adsorption of a nonliving molecular organic conditioning film is the first event in the modification of a solid surface upon its immersion in any natural aqueous environment. The conditioning film has been described by a number of researchers using a variety of techniques. Baier (1972) and Baier and Weiss (1975) have used Multiple Attenuated Internal Reflection (MAIR) IR Spectroscopy and contact angle measurements to show how the solid surface energy is modified by adsorption of organics in human blood and in seawater. Neihof and Loeb (1974) and Loeb and Neihof (1975) have followed formation of the film in seawater by ellipsometry and by microelectrophoresis. Baier (1972) and Tosteson et al. (1978) have discussed the composition of the film and have shown it to consist of an initially adsorbed glycoprotein coating and a subsequent layer of mucopolysaccharide rich adhesive substances.

Neihof and Loeb (1974) and Loeb and Neihof (1975) have shown that the conditioning film is substantially complete in 8 to 10 hours of immersion in seawater. They also demonstrated along with Baier (1975) and DePalma et al. (1982) that the conditioning film masks the original properties of the solid surface. In spite of this masking effect by the conditioning film, Dexter et al. (1975), Fletcher and Loeb (1976, 1979) and Dexter (1976) have shown a correlation between the wettability of the original solid surface and the rate of attachment of the bacterial primary film. The question then arises as to how information about the original surface is transmitted to the attaching bacteria in the presence of the conditioning film. Dexter (1979) suggested that the conditioning film itself provides the means of information transferal. Depending upon the initial surface energy of the solid, as characterized by its wettability, Dexter suggested that the fraction of organic molecules adsorbing may change,

or the conformation of these molecules on the surface may be altered, or the time constant of adsorption may vary or all three. Recently, Little and Zsolnay (1982), using a pyrolsis mass spectrometry technique, presented data which strongly suggest that there is some selectivity in the fraction of the organics that adsorb to several surfaces in seawater.

There is, thus, a need to know more about the nature of the conditioning film and its relation to the details of the initial surface properties of the solid. The techniques that have previously been used to study the conditioning film are all limited in one respect or another. Contact angle measurements show that the surface properties have changed but give little information on the nature or conformation of the film. MAIR spectroscopy provides much information about the composition of the film and its conformation but is applicable only to certain specialized surfaces such as germanium. Electrophoresis is likewise limited to platinum surfaces. Ellipsometry is not surface limited but gives information only on the film thickness -- and that only if the refractive index of the film is known or can be estimated. Pyrolysis mass spectrometry yields information on the distribution of molecular weights of the molecules in the film but at the cost of complete destruction of the film and loss of all information about the orientation of the molecules.

There is, thus, a need for a nondestructive technique which can detect and characterize the conditioning film in real time, as it is forming underwater and on a variety of interesting surfaces ranging from glass and ceramics to metals and polymers. This report will present in some detail our efforts under ONR support to adapt photoacoustic spectroscopy (PAS) to this need. In the following sections we will give an outline of the theory of conventional PAS at the solid/gas interface, the modifications that must be made for the technique to work at the solid/liquid interface, the difficulties that have

been encountered and overcome, the success we have had to date, the known limitations of the technique, and what still remains to be done.

Results from this ONR sponsored work prior to our development of the photoacoustic spectrometer have been published. A series of reprints are included here as an appendix, but those earlier results will not be considered further in the body of this report.

II. THEORY OF PHOTOACOUSTIC SPECTROSCOPY

A. The Physics of Signal Production

The components of a conventional PAS spectrometer for examining a solid surface in air are shown schematically in Figure 1 as first described by Rosencwaig (1977). A beam of monochromatic light from a Xenon arc lamp impinges on the solid surface. The light beam in pulsed by chopping it either electronically or mechanically. The pulsed light is absorbed by the solid surface and converted into heat. The heat is transferred to the boundary layer of fluid (air) in the cell as shown in Figure 2. The boundary layer of fluid expands and contracts in response to the periodic heat flow, thus acting as an acoustic piston producing a periodic pressure pulse in the remainder of the gas in the closed cell. The periodic pressure pulse is detected by a microphone, amplified and recorded as a function of the wavelength of the light by a suitable set of electronics referenced to the pulsed frequency.

The equations describing this process have been given by Rosencwaig (1977) and are outlined for signal production at the solid-gas interface below. Referring to Figure 2 for a cylindrical cell of diameter D and length L, the sample is a disk of diameter D and thickness ℓ. This sample is mounted on a backing material of poor thermal conductivity and thickness ℓ_b. The governing equations for thermal diffusion in the solid are:

In The Sample:

$$\frac{\partial^2\phi}{\partial x^2} = \beta_s^{-1}\frac{\partial\phi}{\partial t} - Be^{\alpha x}(1 + e^{i\omega t}) \qquad -\ell \leq x \leq 0, \qquad (1a)$$

In The Backing:

$$\frac{\partial^2\phi}{\partial x^2} = \beta_b^{-1}\frac{\partial\phi}{\partial t} \qquad -\ell-\ell_b \leq x \leq -\ell \qquad (1b)$$

In The Gas:

$$\frac{\partial^2\phi}{\partial x^2} = \beta_g^{-1}\frac{\partial\phi}{\partial t} \qquad 0 \leq x \leq \ell_g \qquad (1c)$$

where:

$B = \alpha I_o/2k_s$

The subscripts s, b and g refer to sample, backing and gas, respectively.

ϕ = temperature (°C)

t = time (sec)

α = optical absorption coefficient (cm^{-1})

ω = copping frequency (rad sec^{-1})

β_j = thermal diffusivity of material; (cm^2 sec^{-1})

$\beta_j = k/\rho c$ where: k = thermal conductivity (cal/cm sec °C);

ρ density (g cm^{-3}); and c = specific heat (cal/g °C).

Using the above equations with boundary conditions requiring temperature and heat flux continuity at x = 0 and at x = $-\ell$, and requiring the temperature at the cell walls to be ambient, Rosencwaig (1977) gives the solution for Γ, the complex amplitude of the periodic temperature at the solid-gas interface (x = 0) as:

$$\Gamma = \frac{\alpha I_o}{2k_s(\alpha^2-\sigma_s^2)} \left[\frac{(r-1)(b+1)e^{\sigma_s \ell} - (r+1)(b-1)e^{-\sigma_s \ell} + 2(b-r)e^{-\alpha \ell}}{(g+1)(b+1)e^{\sigma_s \ell} - (g-1)(b-1)e^{-\sigma_s \ell}}\right] \qquad (2)$$

where:

$b = k_b A_b / k_s A_s$

$g = k_g A_g / k_s A_s$

$kA = k\sqrt{\omega\rho c/2k} = \sqrt{\omega\rho ck/2}$

thus $g = \sqrt{(\rho ck)_g/(\rho ck)_s}$

$r = (1-i)\alpha/2A_s$

$\sigma_s = (1+i)A_s$

A_j = thermal diffusion coefficient of material j.

$= \sqrt{\omega/2\beta} = \sqrt{\omega\rho c/2k}$ (cm^{-1})

Such a periodic heating of the boundary layer causes this layer of gas to expand and contract periodically, acting as an acoustic piston on the remainder of the gas column in the cell, and producing a periodic pressure signal that is detected by the microphone. Rosencwaig (1977) then proceeds to show that the displacement of the boundary layer of gas due to the periodic heating can be estimated from the ideal gas law to be:

$$\delta_x(t)_g = \frac{\Gamma}{\sqrt{2}\, A_g T_o} \exp[i(\omega t - \pi/4)] \qquad (3)$$

If the rest of the gas in the cell responds adiabatically to this displacement, then the acoustic pressure in the cell can be derived from the adiabatic gas law, PV^γ = constant, and is given by:

$$\Delta P(t)_g = Q \exp[i(\omega t - \pi/4)] \qquad (4)$$

where Q = the complex envelope of the pressure variation

$$= \gamma P_o \Gamma/\sqrt{2}\ell_g A_g T_o \qquad (5)$$

in which γ is the ratio of specific heats from the perfect gas law, and P_o and T_o are the ambient pressure and temperature of the cell. Combining Equations (2) and (5) then yields an explicit but rather messy expression for the complex envelope of the sinusoidal pressure variations detected by the microphone as the PAS signal from the solid-gas interface.

B. The Water Cell Idea

Our proposal was to modify the PAS system to examine adsorptive events at the solid-liquid interface. In order to do this we needed to replace the gas (air) in the cell with water. Our original concept of the PAS water cell system is shown schematically in Figure 3. Initial experiments with this type of cell, however, produced no detectable signal. We then set out, using Rosencwaig's theory as outlined above, to calculate the relative signal strength that might be expected in a water cell with a polyethylene sample as compared to that in an equivalent air cell. First, we assumed that the backing (or sample mounting) material had essentially the same properties as the sample so that b = 1. Equation (2) for the complex amplitude of the periodic temperature fluctuation at the solid/gas interface then simplifies to:

$$\Gamma_{sg} = \frac{\alpha I_o}{2k_s(\alpha^2-\sigma_s^2)} \left[\frac{2(r-1)e^{\sigma_s \ell} + 2(1-r)e^{-\alpha \ell}}{2(g+1)e^{\alpha_s \ell}}\right] \qquad (6)$$

A similar equation can be written for the temperature fluctuation at the solid/liquid interface:

$$\Gamma_{sl} = \frac{\alpha I_o}{2k_s(\alpha^2-\sigma_s^2)} \left[\frac{2(r-1)e^{\sigma_s \ell} + 2(1-r)e^{-\alpha \ell}}{2(w+1)e^{\sigma_s \ell}}\right] \qquad (7)$$

where $w = k_w A_w / k_s A_s$ for the water. Now taking the real part of Equations (6) and (7) (where $\theta = \mathrm{Re}\,[\Gamma]$) the ratio of the real temperature fluctuation at

the solid/liquid interface to that at the solid/gas interface can be written

$$\frac{\theta_{sl}}{\theta_{sg}} = \mathrm{Re}\left\{\frac{\Gamma_{sl}}{\Gamma_{sg}}\right\} = \frac{\frac{1}{(w+1)}}{\frac{1}{(g+1)}} = \frac{(g+1)}{(w+1)} \tag{8}$$

Using the definitions of g and w:

$$\frac{\theta_{sl}}{\theta_{sg}} = \left[\sqrt{\frac{(\rho ck)_g}{(\rho ck)_s}} + 1 \Big/ \sqrt{\frac{(\rho ck)_w}{(\rho ck)_s}} + 1\right] \tag{9}$$

Thus for a given chopping frequency and incident light intensity; and using values of ρ, c and k for polyethylene, fresh water and air at 1 atm pressure and 25°C (see Table I),

$$\frac{\theta_{sl}}{\theta_{sg}} \simeq 0.3 \tag{10}$$

This was encouraging in that replacing the air in the PAS cell with water would only reduce the thermal signal at the interface by about a factor of three.

Returning to Equation (4) we need to make the same type of ratio calculation to determine the relative pressure pulse in the water cell produced by the temperature fluctuation. The displacement of the boundary layer of water in the cell will no longer be found from the perfect gas law, but will be a function of the linear expansion coefficient for water, ν_w, and the temperature variation. Thus, for the water cell,

$$\delta_x(t)_w = \frac{\Gamma_{sl}\nu_w}{\sqrt{2}\, A_w T_o} \exp[i(\omega t - \pi/4)] \tag{11}$$

The expression for the acoustic pressure in the water cell analogous to Equations (4) and (5) for the gas cell is then:

Table I

Properties of Substances at 1 atm pressure and 25°C

	Density ρ ($g\ cm^{-3}$)	Specific Heat C $cal\ (g\ °C)^{-1}$	Thermal Conductivity k $cal\ (cm\ sec\ °C)^{-1}$
Polyethylene	0.92	0.55	5.0×10^{-4}
Water	1.00	1.00	1.4×10^{-3}
Air	1.29×10^{-3}	0.24	5.7×10^{-5}

$$\Delta P(t)_w = Q_w \exp[i(\omega t - \pi/4)] \qquad (12)$$

where

$$Q_w = \nu_w P_o \Gamma_{s\ell} \; / \sqrt{2}\, \ell_w A_w T_o \qquad (13)$$

and $\Gamma_{s\ell}$ is given by Equation (7) for the temperature fluctuation at the solid/liquid interface with b=1. Proceeding as before to take the real part of Q, and setting $\ell_g = \ell_w$ (that is, assuming the cells have identical geometry), then the ratio of the actual pressure variation in the water cell to that in the gas cell is

$$\frac{Q_w}{Q_g} = \frac{\nu_w}{\gamma} \frac{A_g}{A_w} \frac{(g+1)}{(w+1)} \qquad (14)$$

Now taking $\nu_w = 2 \times 10^{-4}\ ^\circ C^{-1}$, $\gamma = 1.4$ and the same values for ρ, c and k for water, air and polyethylene as shown in Table I:

$$\frac{Q_w}{Q_g} = 3.6 \times 10^{-6}$$

This value assumes that the temperature fluctuation at the solid/fluid interface is the same in both cells. We have already shown that the temperature fluctuation in the water cell is only about one third of that in the air cell (see Equation (10)). Taking the reduced temperature fluctuation into account,

$$\frac{Q_w}{Q_g} = (3.6 \times 10^{-6})\ (0.3) = 1.08 \times 10^{-6}$$

and we find that the acoustic pressure in the water cell is expected to be about six orders of magnitude less than that in an air cell with identical geometry and the same light intensity at the interface. The difference is attributed primarily to the small linear expansion coefficient of water, and secondarily to its larger specific heat.

C. Off The Back Side

The comparative calculations performed above were quite discouraging and cast considerable doubt on the feasibility of using PAS in the way we had originally intended. A modification of the experimental arrangement has, however, made it possible to surmount the difficulty and continue with development of the idea. At the Summer, 1980 Gordon Conference on Metallic Corrosion, Strehblow (1980) presented a PAS analysis of the corrosion products on a copper sample. Strehblow divided his PAS cell into two chambers with the divider being the copper sample in the form of a thin foil. The front chamber was filled with water, and the corrosion product film to be analyzed was allowed to develop at the front copper/water interface. On the back side of the sample, however, instead of the backing material shown in Figure 2, was an air chamber containing a microphone (see Figure 4). The copper sample was made thin enough that its thermal diffusion length, μ_{copper} (the inverse of its thermal diffusion coefficient, A) was greater than the physical thickness of the sample as shown in Figure 5. The result was that the thermal signal resulting from periodic absorption of the incident light by the copper and its corrosion product films penetrated through to the copper/air interface and was detected by the microphone in the air chamber.

We quickly verified in our laboratory that this arrangement does work, and the following sections describe our experimental setup and the results obtained.

III. EXPERIMENTAL

The photoacoustic cell for the modified experimental setup (Figure 4) is shown in detail in Figure 6. The body of the cell was machined in four sections from two inch diameter aluminum alloy 6061 rod. The thin sheet samples were

held in place by opposing silicone rubber o-rings. The cell was held together after sample insertion by six socket-head cap screws as shown.

Several materials were tried as samples during the initial phase of our experimental program. First, we reproduced Strehblow's (1980) work on copper. We found, in agreement with his work that a copper foil produced a satisfactory PAS signal, provided that the foil thickness did not exceed 0.004 inches. Commercial brass shim stock produced similar results. The use of aluminum foil, 0.001 inches thick, was less successful. Very little signal was produced by the aluminum foil, probably because the aluminum is a good reflector and does not absorb light very strongly at any wavelength less than 900 nm. A small signal was produced from the aluminum foil when we reduced its reflectivity by etching the surface with 20% HNO_3 at 60°C. We also tried solid surfaces of polytetrafluoroethylene at 0.010 inches thick, and polyvinylfluoride (PVF) at 0.001 inches thick both supplied by E. I. duPont de Nemours, Inc., Wilmington, Delaware; and polyethylene at 0.010 inches thick supplied by Monsanto, Inc., St. Louis, Missouri.

No useable PAS signal was obtained from the polytetrafluoroethylene or polyethylene films because their thickness was greater than the thermal diffusion length in agreement with theory. A weak signal was obtained from the PVF. The problem with the PVF sample was that at 0.001 inches thick, the film transmitted most of the light rather than absorbing it.

The most successful of our initital nonmetallic sample surfaces was Parafilm M™ Laboratory Film (hereafter referred to as Parafilm). This commonly used laboratory film is 0.005 inches thick and produced a consistent,

---

TM: Parafilm M is a Trademark of American Can Company.

relatively strong PAS signal. Parafilm M is a blend of parafin wax with polyethylene and polybutylene. The latter two components give the film its flexibility and elasticity. No special surace preparation was required. Samples could be cut to fit in the cell either before or after adsorption of various organic films to the surface.

Several types of organic films were adsorbed to Parafilm M as follows. A 3 x 4 inch piece of Parafilm was immersed in Lower Delaware Bay water off the College of Marine Studies' pier just inside Roosevelt Inlet for four days. This exposure is known to produce a well-developed primary film of marine bacteria and slime (Dexter, 1979). The Parafilm was then air dried, cut into a 2 centimeter diameter disk shaped specimen and mounted in the cell. An organic hydrocarbon film was adsorbed to Parafilm by immersing a pre-cut sample into undiluted 1-iodonapthalene for four hours. A film of a common commercial hand lotion was applied to one side of a pre-cut Parafilm specimen with a cotton swab and spread to a nominal thickness of 0.001 to 0.002 inches before mounting the sample in the cell. The enzyme, tyrosine, was adsorbed to the parafilm by placing one to two ml of a solution of the crystalline enzyme in methanol onto the surface of the film and drying in air for 3 hours. After the methanol had evaporated, a visible film of the enzyme remained on part of the Parafilm surface.

Incident light from the Xenon arc lamp was passed through a monochromator and pulsed by a mechanical chopper as shown in Figure 7. This incident light beam entered the cell through a UV quality, 2 mm thick sapphire window held in place by GE silicone cement. In order to maximize the incident light intensity, the optical system (Figure 7) was aligned so that maximum light entered the monochromator. The lenses used were all UV grade quartz or Spectrasil B. Back reflection of light from the flat sapphire window was minimized by tilting

the cell so that its cylindrical axis was 5 to 10° from the light path leaving the monochromator. This slight tilting of the cell not only allowed more light to strike the sample surface, but also minimized internal reflections which may produce interferring signals.

The PAS signal was detected by a B & K (Bruel and Kjaer) model 4155 prepolarized condenser microphone with model 6169 preamplifier. The microphone output voltage contains not only the desired PAS signal, whose frequency is that of the pulsed light beam, but also extraneous signals of both acoustic and electronic origin having a wide range of frequencies. In order to extract and record only the desired PAS signal, the frequency at which the mechanical chopper pulses the incident light beam is used by the lock-in amplifier as a reference. The lock-in amplifier rejects all input signals with frequencies different from the reference value and produces a DC output voltage equal in magnitude to that of the input signal at the reference frequency.

Low signal-to-noise ratio has been a constant problem in this work to develop PAS as a useful analytical tool for looking at organic film formation under water. In order to increase the signal-to-noise ratio, we have maximized the incident light intensity as described above, increased the microphone sensitivity and reduced the background noise. Microphone sensitivity was increased 12 dB by switching from our original Knowles model 4159 electret microphone to the B & K microphone mentioned above. This resulted in a similar increase in the signal-to-noise ratio. The penalty is an increase in the price of the microphone from $20 to $1,200.

The PAS signal produced by the lock-in amplifier was greatest for samples having strong absorption peaks within the 200 to 900 nm range. Carbon black, with a signal-to-noise ratio of nearly 1000:1 is a strong absorber at all wavelengths within the above range and was used routinely as a reference

material for obtaining the power spectrum of the Xenon arc lamp. Parafilm M had a signal-to-noise ratio between 50:1 and 100:1. The copper and brass foils had values near 50:1, and all other sample surfaces tried had values of less than 10:1.

The variations in PAS signal produced by the organic films we wish to study are likely to be relatively small. In order to distinguish such small variations in signal from the background noise, the signal-to-noise ratio should ideally be 1000:1. Much can still be done with a ratio of 100:1 as was frequently the case with Parafilm but rarely is useful information available when the signal-to-noise ratio drops below the 40 to 50:1 range. In the latter case, the small variations in the PAS signal which contain most of the useful data become indistinguishable from the background noise.

Several methods of background noise level reduction were tried. Mechanical vibrations at the chopping frequency of 40 Hz, or having harmonics at the chopping frequency, were found to be the major external contributors to the background noise level. The following three principal sources for such vibrations were identified and are listed in order of increasing severity: door slams, the laboratory building's heating and cooling system, and the mechanical chopper. Most other sources of external noise were at frequencies far enough removed from the chopping frequency that they were filtered out by the lock-in amplifier. The cell was isolated as much as possible from the three troublesome sources of vibration listed above by supporting it on a bed of sand, which is a poor transmitter of low frequency vibrations.

In addition, the cell was isolated from general room noise, including that from voice communications, by placing it inside a foam lined box having only two holes--one to admit the incident light beam, and the other for the microphone cord. This foam lined chamber effectively reduced high frequency

inputs but made far less overall difference than the sand bed because the low frequency noise was more significant.

Internal electronic noise came mostly from the microphone itself and its built-in preamplifier. The lock-in amplifier contributed very little noise. One experiment was performed late at night with no people other than the authors and the facilities engineer in the building (no door slams) and with all machinery in the building shut off. The background noise under these "quiet building" conditions was about 55 dB and was mostly attributed to the electronic noise of the microphone and preamplifier. The total background noise during daytime hours typically runs between 60 and 70 dB.

The photoacoustic spectrum for a given sample surface was obtained by scanning the 200 to 900 nm wavelength range at a rate of 20 nm/min. The monochromator was driven at this rate by a synchronous motor. The PAS signal in volts from the output of the lock-in amplifier was recorded on a strip chart recorder whose chart speed was correlated with the scan rate of the monochromator.

At the start of each day's work, a carbon black spectrum was run to obtain the power spectrum of the Xenon arc lamp over the 200 to 900 nm wavelength range. The power spectrum proved to be quite consistent from day to day. Raw data from the scans of voltage signal vs. wavelength for the Parafilm samples with various organic layers contained three components: the power spectrum of the lamp, PAS signal contributed by the Parafilm substratum, and the desired PAS signal from the organic film. In order to plot the PAS signal from the organic film alone, the other two components were removed as follows. Data points for the carbon black spectrum to be used as a reference were picked off the strip chart recording at 10 nm intervals. The sample spectrum was then scaled up or down to the carbon black reference by multiplying it by

the ratio of the carbon black to sample signals at 460 nm. The wavelength of 460 nm was chosen as it is the location of the strongest peak in the region of the power spectrum having the most significant PAS signal. After scaling, the carbon black spectrum was subtracted point by point from that of the sample spectrum. The resulting difference spectrum was then plotted as relative PAS signal vs. wavelength. The PAS signal contributed by the Parafilm substratum could be subtracted out by repeating the above procedure. In practice, however, it was common to combine the two subtractions into a single operation. This was done by treating the raw spectrum from a clean Parafilm sample as a reference. The new reference spectrum contained both the power spectrum of the lamp and the Parafilm contributions to the PAS signal. Thus, by using it as the reference spectrum in the above procedure, both components were removed together.

Raw data were taken over the full 250 to 900 nm range. The reduced spectra, however, were usually plotted only up to 700 nm. This is because the major changes in PAS signal produced by the organic films were in the UV and visible portions of the spectrum, and because the rapid changes in the power spectrum of the lamp with wavelength in the 700 to 900 nm range made that data difficult to reduce.

IV. RESULTS

The raw data of PAS signal in volts vs. wavelength of incident light from a carbon black sample in a cell containing air are shown in Figure 8. These data represent the power spectrum of the Xenon arc lamp, and the small jagged peaks that appear superimposed upon the main features of the spectrum represent the background noise level. A similar set of raw data from a clean Parafilm sample is shown in Figure 9. Before subtracting the power spectrum of the

lamp (Figure 8) from the raw Parafilm data (Figure 9) to get the PAS signal from the Parafilm itself, the two sets of raw data were smoothed. The smoothing process was used to remove both minor background fluctuations as well as the occasional large, erratic and easily identified singular inputs of extraneous signal resulting from doors slamming and machinery noise.

Smoothed raw data for carbon black and Parafilm are shown together in Figure 10 along with the PAS signal from the Parafilm itself obtained from the two curves above it by the procedure described in the previous section. Note that the sharp spike, which was identified with a door slam, at 300 nm on the Parafilm spectrum in Figure 9 has been smoothed out in Figure 10. The PAS signal contributed by the Parafilm has two broad absorption bands. The first is centered at 370 nm in the near ultraviolet, and the second at 530 nm in the visible green. This correlates well with the slightly purple tint of the translucent Parafilm as it appears to the naked eye. These two absorption bands can also be recognized in the smoothed raw Parafilm data by making a point by point comparison of the top two curves in Figure 10.

Smoothed raw data for four organic films on a Parafilm substratum are shown in Figures 11 through 14. These data were all taken with air in both halves of the PAS cell. The data for the seawater organic film and the hand lotion (Figure 11 and 13) were taken while the respective films were still moist. The data for the Tyrosine amino acid and 1-iodonaphthaline, however (Figures 12 and 14), were taken on the dry film. PAS data were also taken on the seawater organic film with water in the front half of the cell. The PAS signal was basically the same, but reduced 5 to 10% in intensity.

Each of the spectra in Figures 11 through 14 was reduced to obtain the PAS signal attributable to the organic film alone. This was done in each case by subtracting the smoothed raw spectrum containing both the lamp and the

Parafilm contributions from the properly scaled and smoothed organic film on Parafilm spectrum. The two smoothed raw spectra and the reduced data for the seawater organic film are shown in sequence in Figure 15. Regions of the reduced spectrum showing positive data represent wavelengths of light at which the organic film has enhanced the photoacoustic signal of the substratum. Those regions in which the reduced data are negative represent wavelengths at which the organic film has decreased the photoacoustic signal of the substratum, while points on the reduced spectrum having zero or near zero values represent wavelengths at which the organic film has a neutral effect.

The reduced data (lower curve) in Figure 15 show that the organic film has an absorption band in the ultraviolet at 250 to 290 nm, followed by a region from about 300 to 400 nm in which the signal is decreased, and then a broad area of mild signal enhancement across the visible range from 400 to 650 nm. The absorption peak in the UV is the most prominent feature of the seawater organic curve and is readily observed in the smoothed raw data. The other two features are less obvious from the raw data.

The reduced data from all four organic films investigated are shown together in Figure 16 starting with the seawater organic film data on the top. The Tyrosine amino acid and the hand lotion both display the same three general features that were seen for the seawater organic film. The UV peak in each of the latter two is less prominent than for the seawater film, and the region of decreased signal is somewhat broader and deeper. In the case of the Tyrosine, the enhancement in the visible portion of the spectrum is both reduced and more erratic than that of the seawater film.

The data for the 1-iodonaphthalene film are quite different from the others. The absorption band in the UV is absent and the enhancement in the visible is the most pronounced.

V. DISCUSSION

This research program has demonstrated that one can use the technique of photoacoustic spectroscopy to detect the presence of organic films on a variety of types of solid surfaces under water in real time. This section of the report will be devoted to a discussion of:

1. The significance of the data presented in the previous section.
2. The apparent capabilities and limitations of photoacoustic spectroscopy as a tool with which to study organic films at the solid-seawater interface.
3. The work remaining to be done before photoacoustic spectroscopy can be used as a scientific tool in studying the early stages of biofilm formation.

It is clear from the data presented in Figures 8 through 16 that the PAS signature of the Parafilm surface is changed by the presence of an organic film. This fact alone means that it is possible to detect the adsorption of an organic film. The question that arises, however, is: How much more than the mere presence of a film can be discerned from the PAS spectra in Figure 16? Can the various organic films be distinquished one from another? In order to answer this question, we must return first to the raw data in Figures 8 and 9 and ask: How much of the fine structure in these figures is significant and how much is merely background noise? Some of the fine structures could be associated with specific inputs of noise as already mentioned concerning the spike at 300 nm on Figure 9. Other features could be identified as noise due to their irreproducibility in successive runs under the same conditions. Examples of this type of noise are: 1) the fine structures of the peak centered at about 400 nm on Figure 9, and the sharp secondary peak at 490 nm on the same figure. Note that these features have been removed from the

corresponding smoothed curve of Figure 10. In contrast to these noise features are the four peaks located between 680 and 770 nm on Figures 8 and 9. These are significant but are part of the power spectrum of the lamp.

In the reduced Parafilm data (lower curve in Figure 10) the two major absorption bands centered at 370 and 530 nm are real and reproducible. The detailed shapes of the two peaks, however, are probably not significant. Minor variations in the shape of a peak in the reduced data are particularly suspect in regions where the slopes of the two parent curves are steep. In the region from 450 to 500 nm in Figure 10, for instance, the slopes of both the carbon black and Parafilm curves are large. In such a case, even a slight lack of synchronization between the strip chart recorder and the monochromator drive motor can cause a secondary peak in the reduced data to appear or disappear, or a peak shape to change.

Returning now to Figure 16, the top three spectra all have the same major features. They all have a peak in the ultraviolet followed by a region in which the PAS signal is suppressed by the organic film and then a broad low level increase in signal through the visible range. The seawater film gives the most pronounced peak in the UV, and the Tyrosine shows the least consistent enhancement in the visible. The spectrum for 1-iodonaphthalene in Figure 16 is clearly different from the other three. The peak between 250 and 300 nm is missing, and 1-iodonaphthalene could be distinquished on the basis of that fact alone. The more important question is whether the seawater organic, Tyrosine and hand lotion can be identified by a unique PAS signature. At first glance, the answer appears to be yes. Such a distinction, however, would have to be based on the fine structure of their respective spectra rather than the major features. The fact that the major features of the seawater organic and the Tyrosine are similar is not surprising because

Tyrosine is an amino acid of which there are many present in seawater. The fine structure that would appear to distinquish Tyrosine from seawater is: first, the shift in the UV peak location from 250 to 270 nm and its decrease in size; second, the greater breadth in the region over which signal strength is diminished, and third, the weaker and more erratic enhancement in the visible. The ability to successfully distinguish between two organics that are inherently similar will depend upon the reproducibility of features such as these, and yet these are precisely the type of features that are most likely to be artifacts caused by instrumental difficulties. Based on the data presented, therefore, the question as to whether the top three organics in Figure 16 can be positively distinguished from their PAS spectra alone cannot yet be answered. Further work will be required to see if the fine structure of the spectra can be made reproducible.

We know now that PAS can be used to detect organic films, and with some further work, may be able to reliably distinguish between the broad types of organic films in Figure 16. None of these films, however, are particularly interesting from a scientific point of view. The important scientific question is: Can PAS be used to identify and study the adsorption of specific organic films that are important in the early stages of biofilm formation in seawater? We have spent considerable time over the past several years in developing the instrumentation and methodology to the point where we can now address this question in a meaningful way. We have shown that the original concept of signal detection by a hydrophone in the water side of the PAS cell will not work. As an alternative, we have shown that most substratum materials of interest can be made thin enough that the PAS signal penetrates through the sample and can then be detected by a microphone placed in an air chamber on the reverse side of the sample. We have shown that this system is versatile

enough to work regardless of whether the front side of the PAS cell contains air or water. This gives one the option of studying the organic films either dry or wet, or even under wet/dry cycling conditions.

The system is also versatile enough that it is not limited to only a few specific solid surfaces. It will work on any metal surface that is not highly reflective. Highly polished or silvery colored metal surfaces are the most difficult to analyze because they do no absorb light strongly enough to produce a PAS signal. Such surfaces could probably be studied if they were given a prior oxidation or etching treatment to reduce their reflectivity. Polymeric surfaces can be studied as long as the samples are made thinner than the thermal diffusion length of the material. For many polymers, this may require the film to be so thin that there is some question as to whether the film would be rigid enough to support the acoustic piston which produces the PAS signal. This problem can most likely be solved by using a thin metallic foil such as copper as a backing material to provide the needed rigidity. The contribution of the backing material to the total PAS signal can then be subtracted out as described earlier.

Another possible limitation in the use of thin polymeric films as substrata for PAS experiments is that many of the polymers of interest may be transparent over the entire 200 to 900 nm spectral range. A substratum that achieves nearly 100% transmissivity (or reflectivity) will produce no PAS signal because insufficient light will be absorbed. In most cases this will not be a problem provided that the organic films adsorbing to the surface do absorb light. It is usually the organic film we wish to study rather than the solid surface on which the film adsorbs.

The PAS system we have developed is now ready for a critical test to see if it can be used in studying the early stages of seawater biofilm formation.

The four day seawater film for which we have presented data in Figure 15 and 16 is too well developed and has too many components to provide much scientific information. That film was chosen for our initial experiments just to find out whether a fully developed seawater film could be detected at all. The need now is to become much more specific. In this regard, we intend to run a series of critical experiments by about the end of 1982. We will ask four specific questions as follows:

1. Can PAS tell the difference between a nonliving conditioning film and a well developed primary film.

To answer this question we will adsorb a seawater conditioning film in the absence of bacteria. Microorganisms will be removed from the water by millipore filtration, and a PAS spectrum taken on the conditioning film only. This data will be compared to that of Figure 15 to see if there is any reproducible difference.

2. Can PAS be used to study the buildup of a conditioning film with time.

Loeb and Neihof have shown that seawater conditiong films are complete in 8 to 10 hours after initial immersion of the substratum. Film formation in the absence of bacteria (as in Question 1 above) will be allowed to take place for 1, 2, 4 and 8 hours. The PAS spectra resulting from these films will be analyzed to see if there are differences.

3. Can PAS distinguish between several well characterized organics with known sharp bands?

Three or four such organics will be adsorbed and the PAS spectra analyzed to see if the known structure is observed.

4. Can PAS distinguish between various dissolved seawater organic fractions based on molecular weight or other chemical criteria.

Three different sterile seawaters will be prepared, each having a different fraction of dissolved organics based on molecular weight (e.g. less than 20,000 only, or greater than 200,000). The PAS spectra from the conditioning films formed in these waters will be analyzed for any characteristic structure.

We intend to continue developing and using PAS as a scientific tool only if we obtain positive and reproducible results in the experiments outlined above. If PAS shows no consistent ability to distinguish between the various organics in the above tests, then it will not be useful as a scientific tool and we will discontinue development of it.

VI. REFERENCES

Baier, R. E., 1972. "Influence on the Initial Surface Condition of Materials on Bioadhesion," in Proc. Third Intl. Congr. on Marine Corrosion and Fouling, National Bureau of Standards, Gaithersburg, MD, October, 1972, p. 633. See also: R. E. Baier, 1970. "Surface Properties Influencing Biological Adhesion," in Adhesion in Biological Systems, R. S. Manly, editor, Academic Press, New York, p. 15.

Baier, R. E., 1975. "Applied Chemistry at Protein Interfaces," in Applied Chemistry at Protein Interfaces - Advances in Chemistry Series 145, American Chemical Society, Washington, DC, p. 1.

Baier, R. E. and Weiss, L., 1975. "Demonstration of the Involvement of Adsorbed Proteins in Cell Adhesion and Cell Growth on Solid Surfaces," in Applied Chemistry at Protein Interfaces - Advances in Chemistry Series 145, American Chemical Society, Washington, DC, p. 300.

DePalma, J. A., King, R. W., Formalik, M., Meyer, A. E. and Baier, R. E., 1981. "Analysis of Primary Films Accumulated During Marine Fouling Program," Arvin/Calspan Final Technical Report to D. W. Taylor Naval Ship R & D Center, Annapolis, MD, October 1, 1981.

Dexter, S. C., Sullivan, J. D., Williams, J. and Watson, S. W., 1975. "Influence of Substrate Wettability on the Attachment of Marine Bacteria to Various Surfaces," Applied Microbiology, 30, p. 298.

Dexter, S. C., 1976. "Influence of Substrate Wettability on the Formation of Bacterial Slime Films on Solid Surfaces Immersed in Natural Sea Water," in Proc. Fourth Intl. Congr. on Marine Corrosion and Fouling, Juan-Les-Pins, Antibes, France, June, 1976, p. 137.

Dexter, S. C., 1979. "Influence of Substratum Critical Surface Tension on Bacterial Adhesion - In Situ Studies," J. Colloid and Interface Sci., 70, p. 346.

Fletcher, M. and Loeb, G. I., 1976. "The Influence of Substratum Surface Properties on the Attachment of a Marine Bacterium," in Colloid and Interface Science - Vol. III, M. Kerker, editor, Academic Press, New York, p. 459.

Fletcher, M. and Loeb, G. I., 1979. "Influence of Substratum Characteristics on the Attachment of a Marine Pseudomonad to Solid Surfaces," Appl. Env. Microbiol., 37, p. 67.

Little, B., and Zsolnay, A., 1982. "Chemical Characterization of Fouling Films with Pyrolysis Mass Spectrometry," submitted to J. Anal. Chem.

Loeb, G. I. and Neihof, R. A., 1975. "Marine Conditioning Films," in Applied Chemistry at Protein Interfaces, Advances in Chemistry Series 145, American Chemical Society, Washington, DC, p. 319.

Neihof, R. A. and Loeb, G. I., 1974. "Dissolved Organic Matter in Seawater and the Electric Charge of Immersed Surfaces," J. Mar. Res., 32, p. 5.

Rosencwaig, A., 1977. "Solid State Photoacoustic Spectroscopy," in Optoacoustic Spectroscopy and Detection, Yoh-Han Pao, editor, Academic Press, New York, p. 194.

Strehblow, H. H., Sander, U. and Dohrmann, J. K., 1980. "In Situ Photoacoustic Spectroscopy of Thin Oxide Layers on Metal Electrodes - Copper in Alkaline Solution," Poster presentation at the July, 1980 Gordon Conference on Metallic Corrosion, New London, New Hampshire.

Tosteson, T. R., Tsai, R. and Corpe, W. A., 1978. "The Composition of Surface Active Macromolecules from Natural Seawater, Micro-organisms and Other Marine Sources," Final Report to the National Science Foundation on Contract: SER 76-08935, September, 1978.

VII. ACKNOWLEDGMENTS

This work was supported by the Oceanic Biology Program of the Office of Naval Research under Contract No. N00014-77-C-0064 and by a grant from the University of Delaware Research Foundation. Development of the PAS instrumentation and water cell were done by K. E. Lucas.

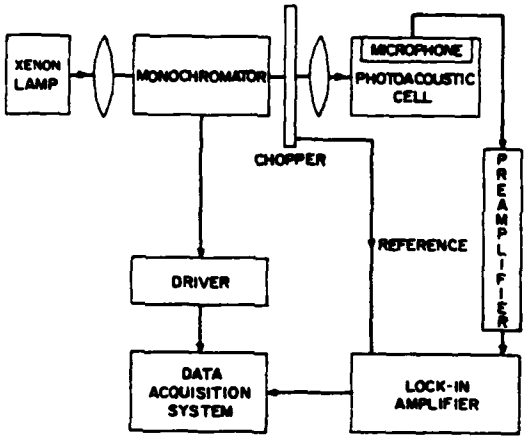

Figure 1. Block Diagram of a Typical Photoacoustic Spectrometer after Rosencwaig (1977).

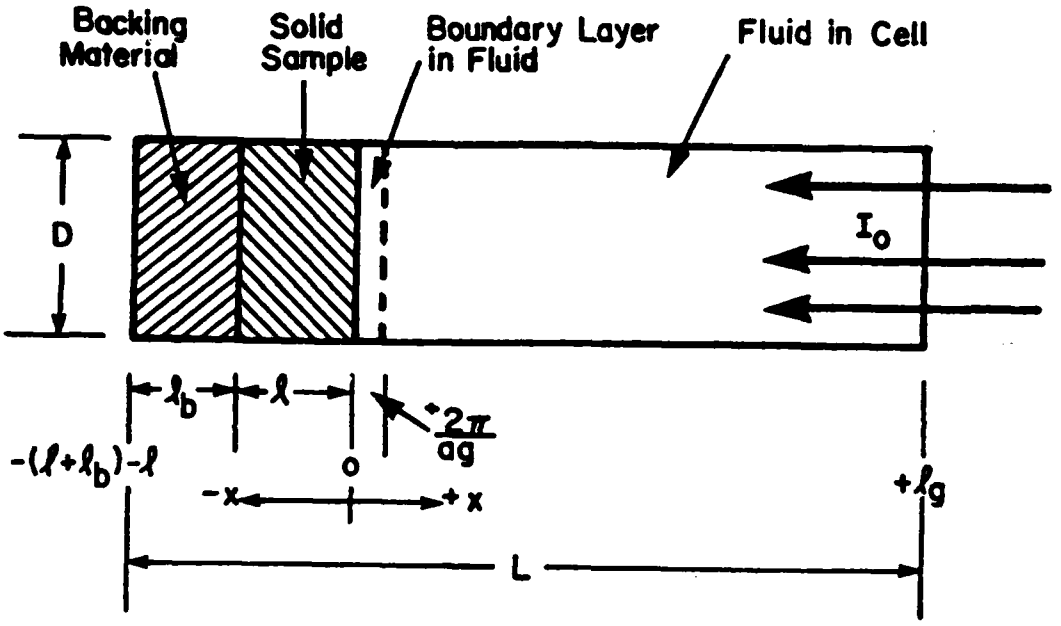

Figure 2. Longitudinal Cross-Section of a Simple Cylindrical Photoacoustic Cell Showing the Important Cell Dimensions.

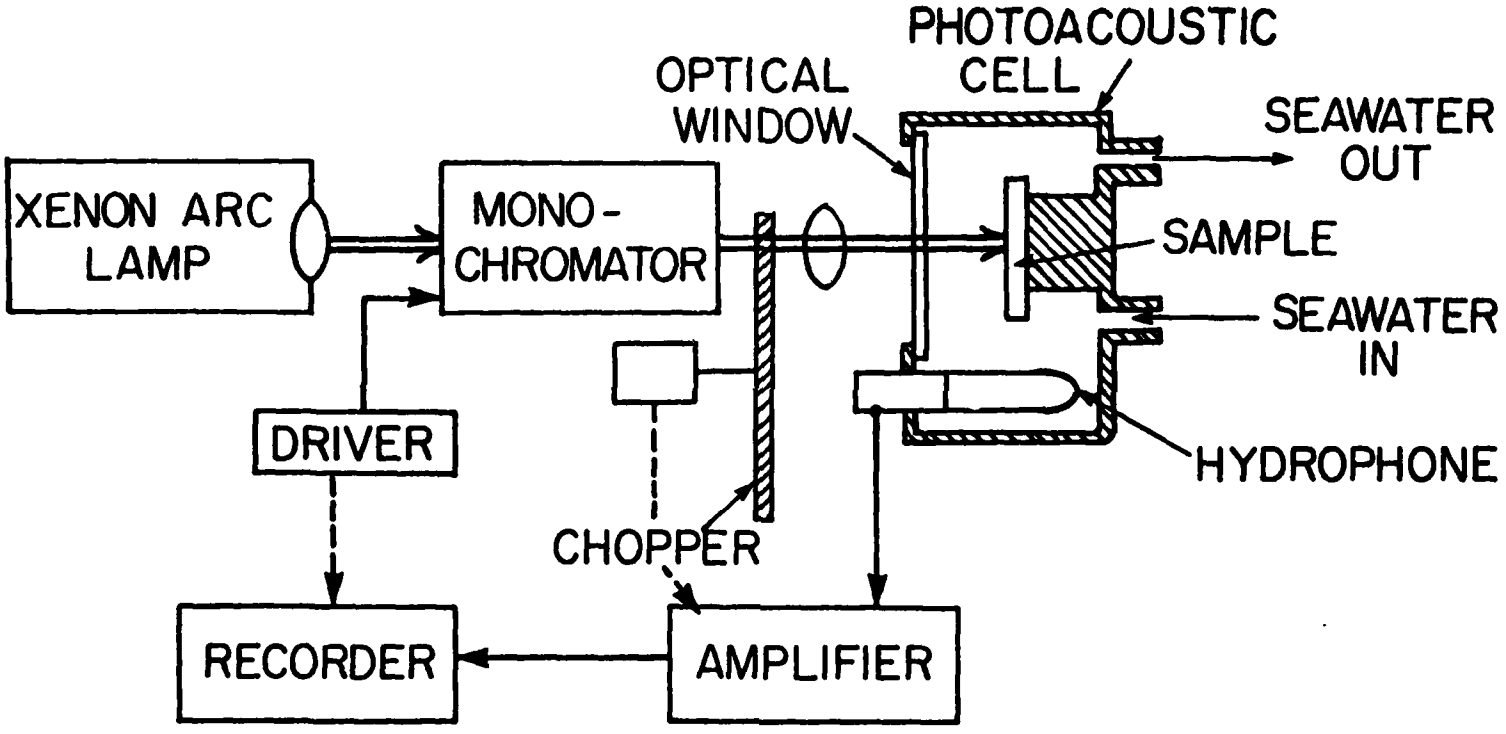

Figure 3. Block Diagram of a Photoacoustic Spectrometer Using a Water Filled Cell with Hydrophone Detector.

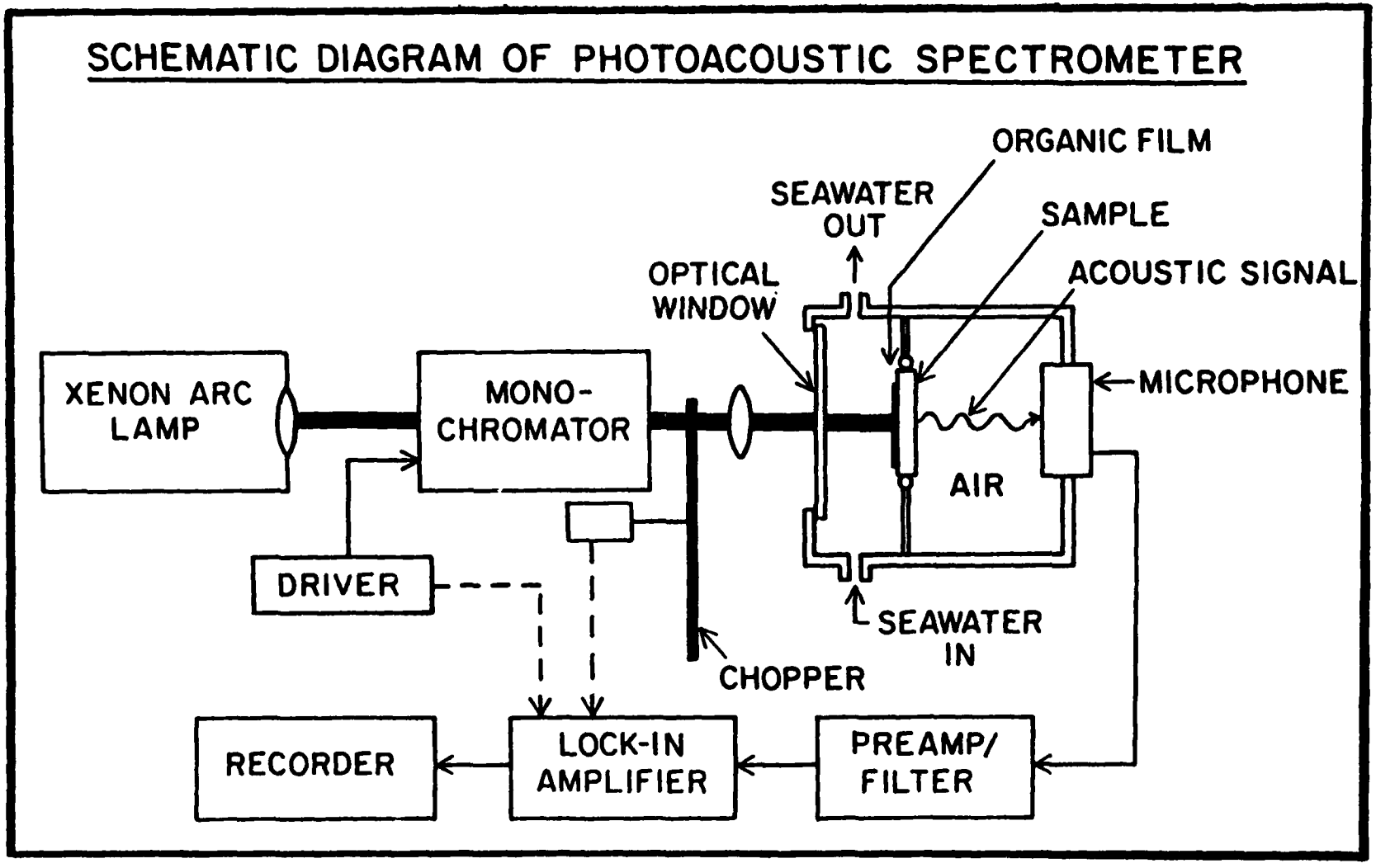

Figure 4. Photoacoustic Spectrometer using a Compound Cell having Water in the Front Chamber and Air or Some Other Gaseous Fluid in the Back Chamber and a Microphone Detector.

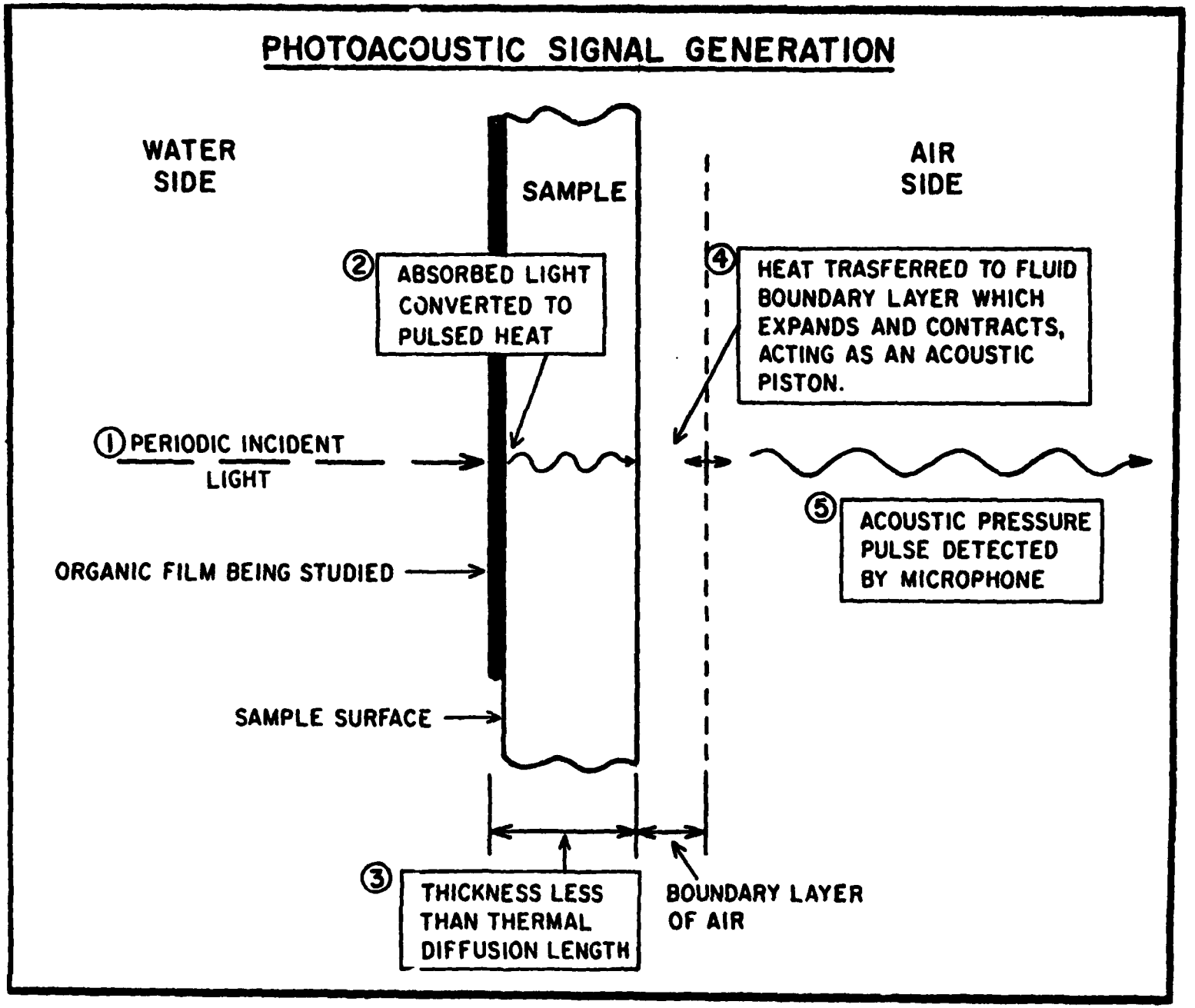

Figure 5. Photoacoustic Signal Generation for the Cell Depicted in Figure 4. The Sample Thickness must be Less than its Thermal Diffusion Length.

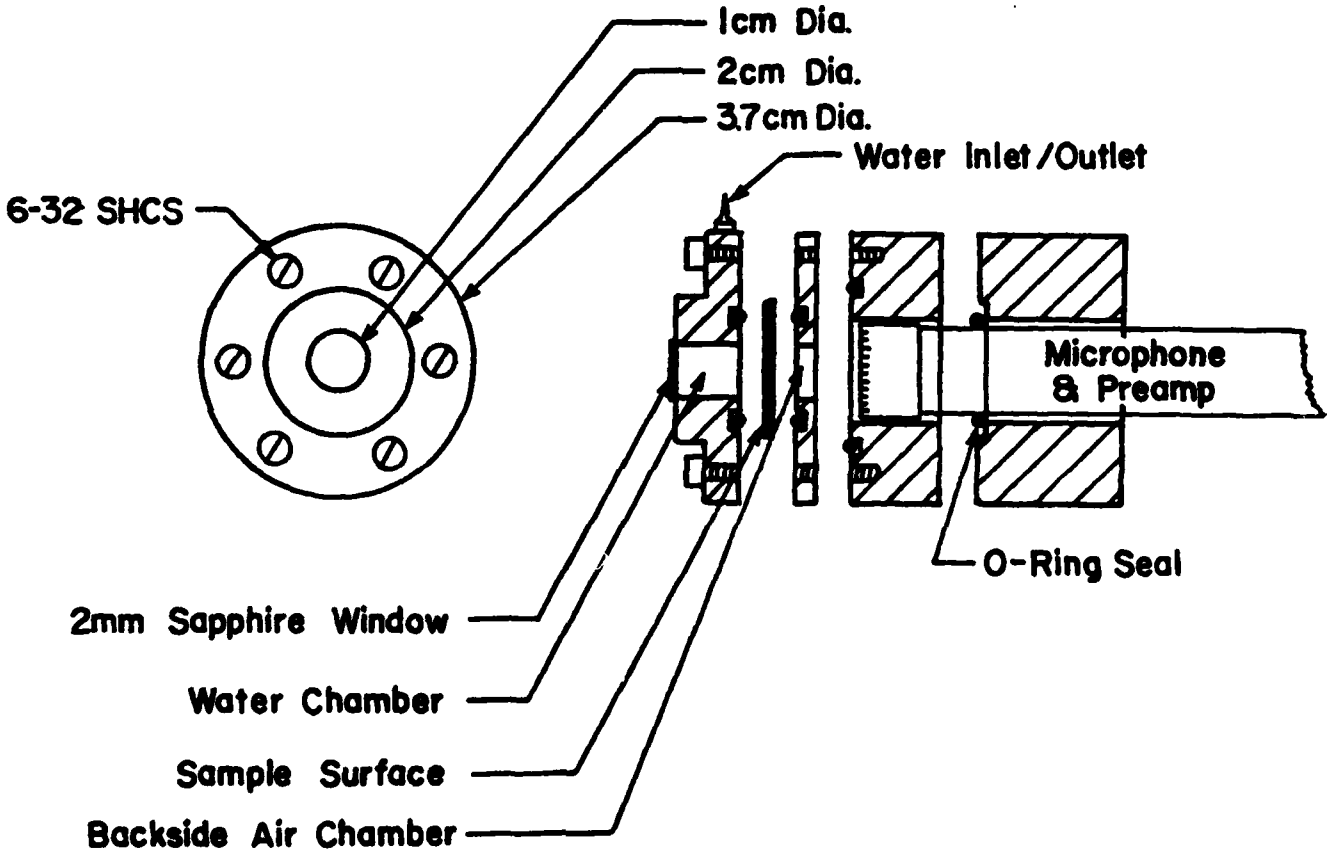

Figure 6. Construction of the Compound Cell Shown in Figure 4.

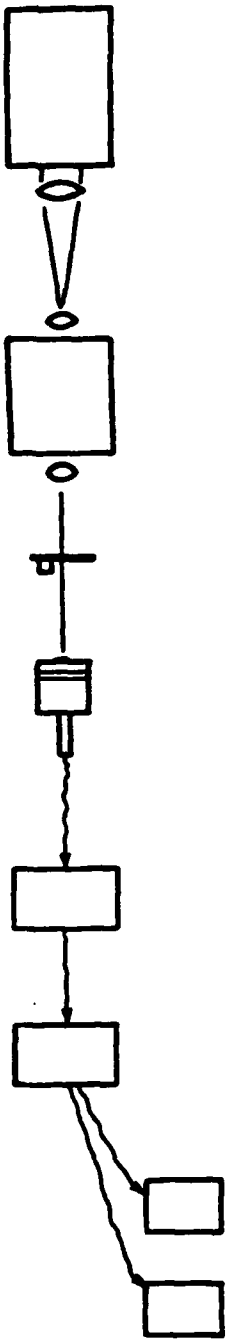

Xenon Arc Lamp	Conrad-Hanovia 1000W #976C
Condenser Lenses (2)	Melles Griot f100, 75mm Dia. Fused Qtz.
Entrance Lens	Melles Griot f50, 25mm Dia Spectrasil B
Monochromator	Kratos/Schoeffel GM252
Exit Lens	Melles Griot f80, 25mm Dia Spectrasil B
Mechanical Chopper	Bentham #218
Window & PAS Cell	Melles Griot Sapphire 25mm Dia., 2mm thick
Microphone	Bruel & Kjaer #4155 prepolarized
Preamp & Filter	Ithaco #425 & #4113
Lock-in Amplifier	Ithaco #393
Chart Recorder	Hewlett Packard #7100B
Oscilloscope	Tectronix #547

Figure 7. Mechanical, Optical and Electrical Components of the Photoacoustic Spectrometer.

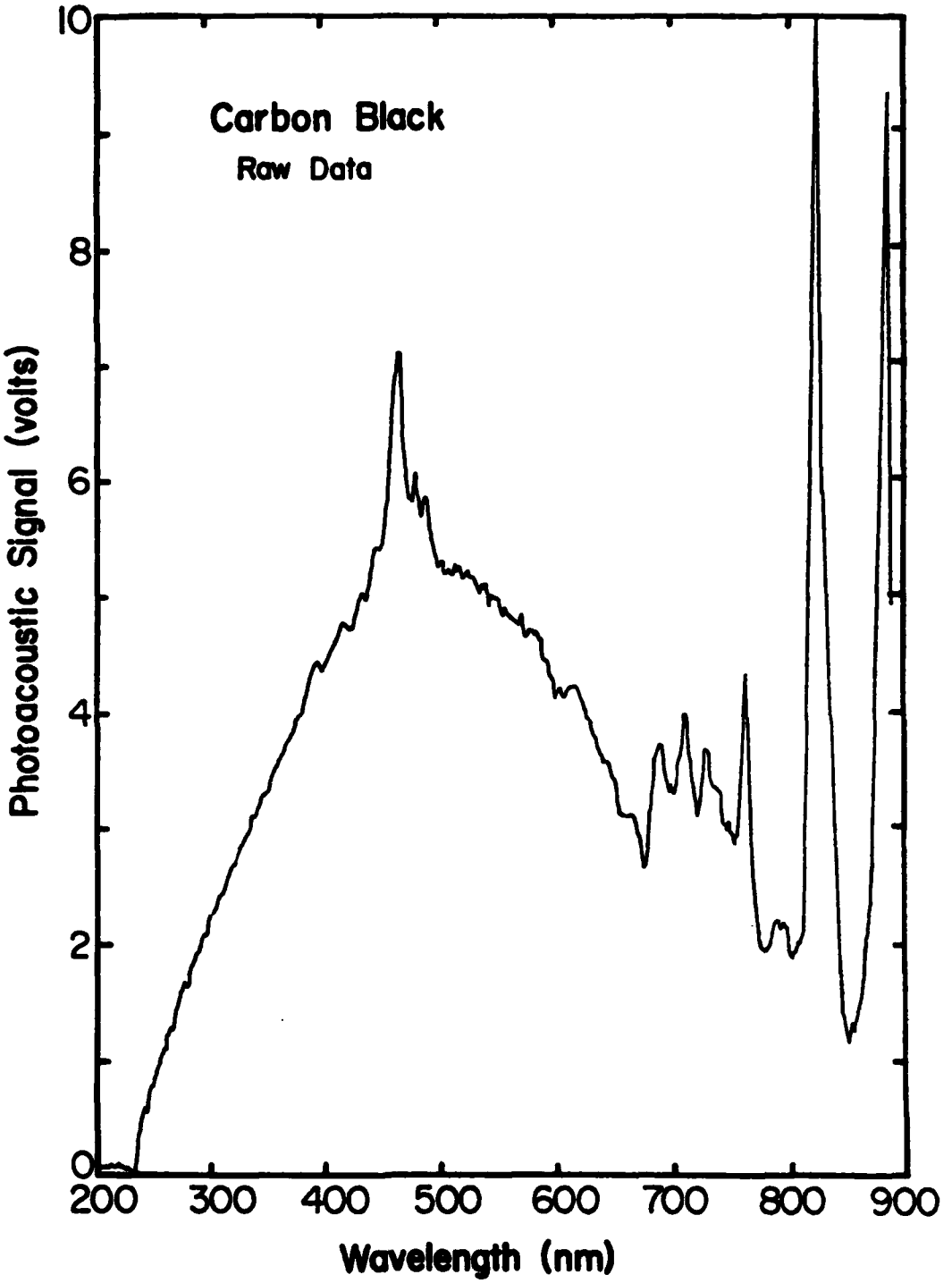

Figure 8. Raw PAS Signal on Carbon Black Representing the Power Spectrum of the Xenon Arc Lamp.

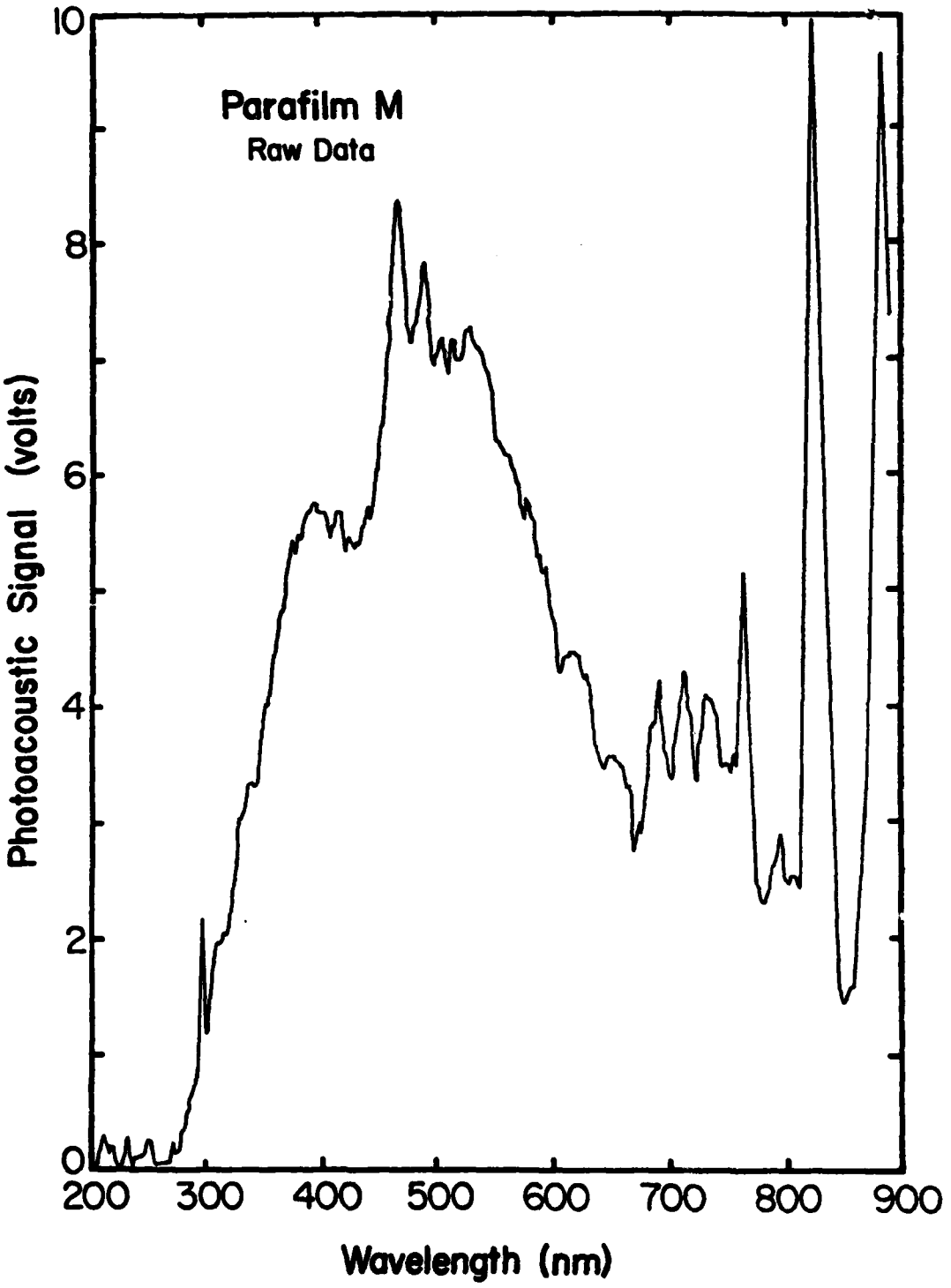

Figure 9. Raw PAS Spectrum for a Parafilm Sample.

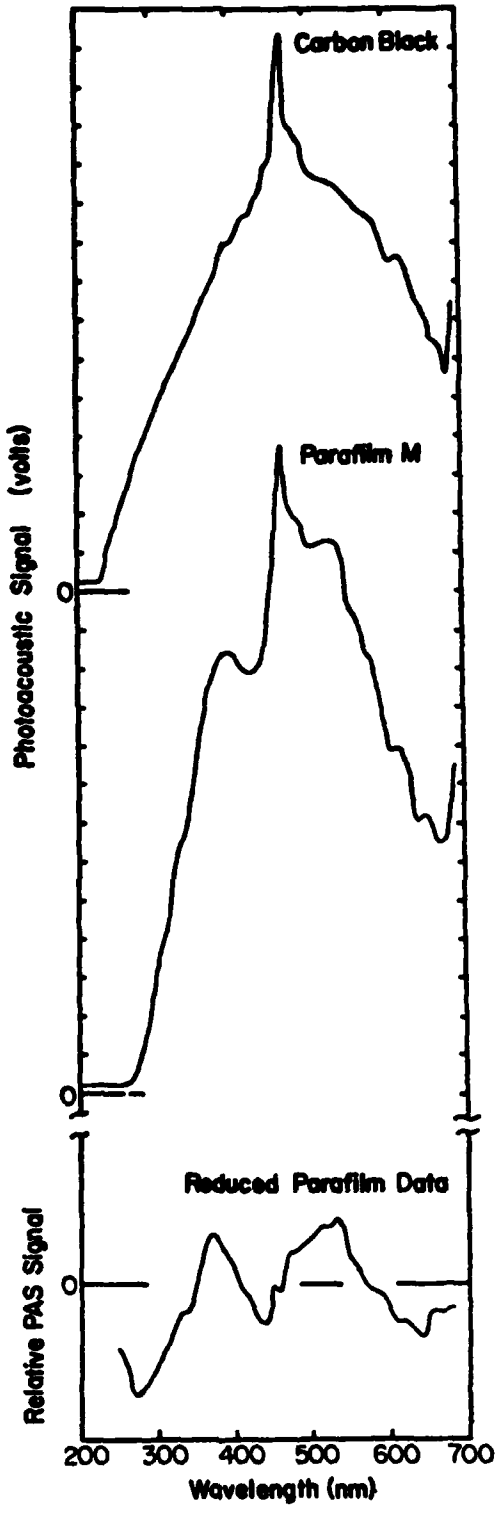

Figure 10. Smoothed Raw Data for Carbon Black and Parafilm and the Reduced Parafilm Spectrum Showing Absorption Bands Centered at 370 and 530 nm.

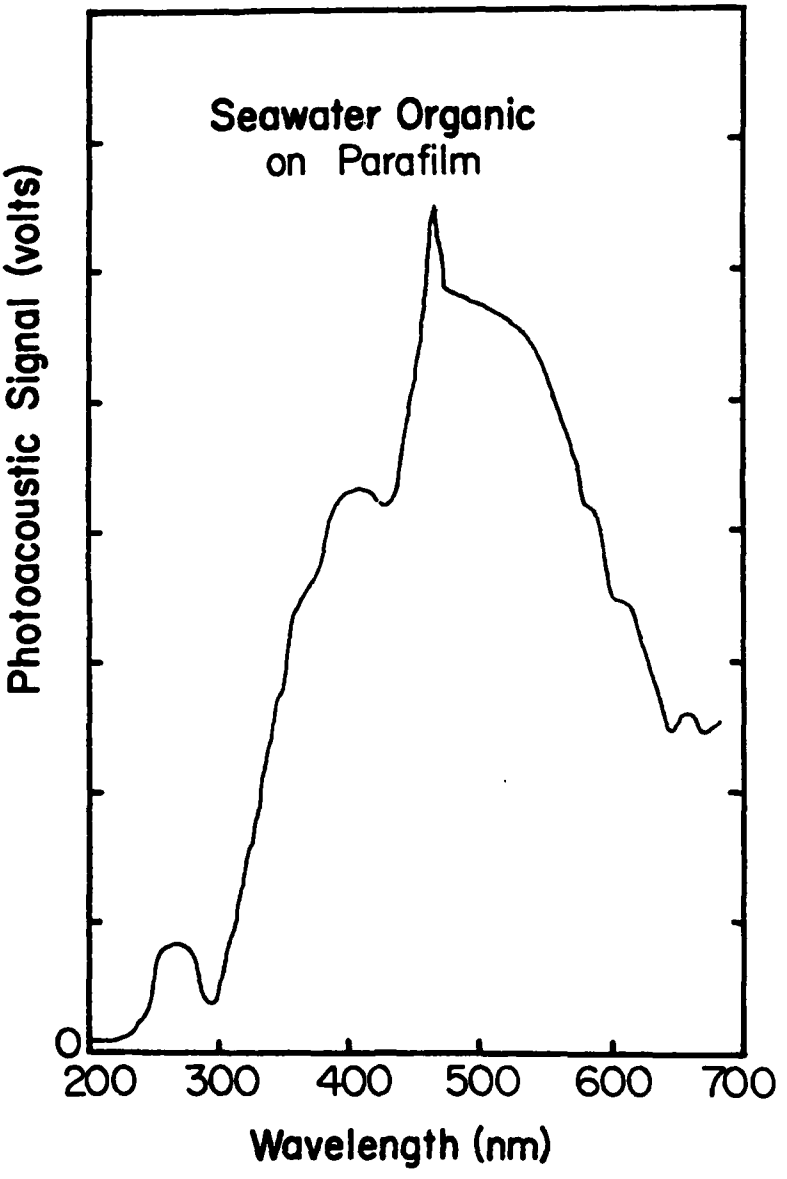

Figure 11. Smoothed Raw PAS Spectrum for a Four-Day Seawater Primary Film on Parafilm.

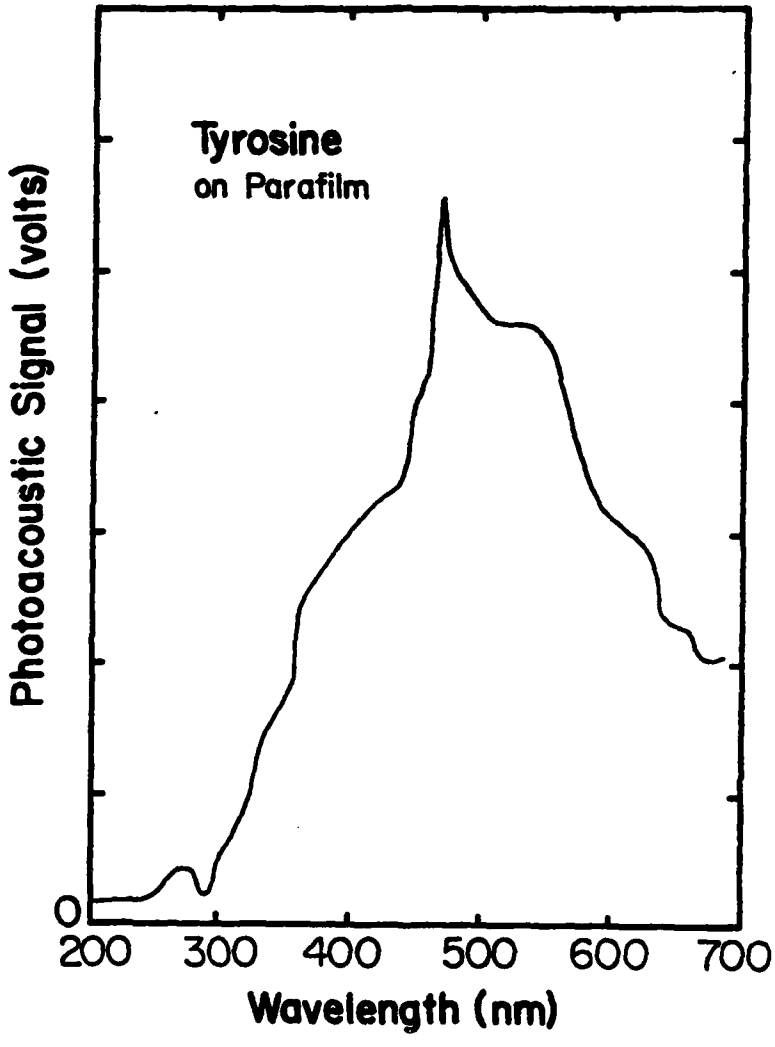

Figure 12. Smoothed Raw PAS Spectrum for the Amino Acid, Tyrosine, on Parafilm.

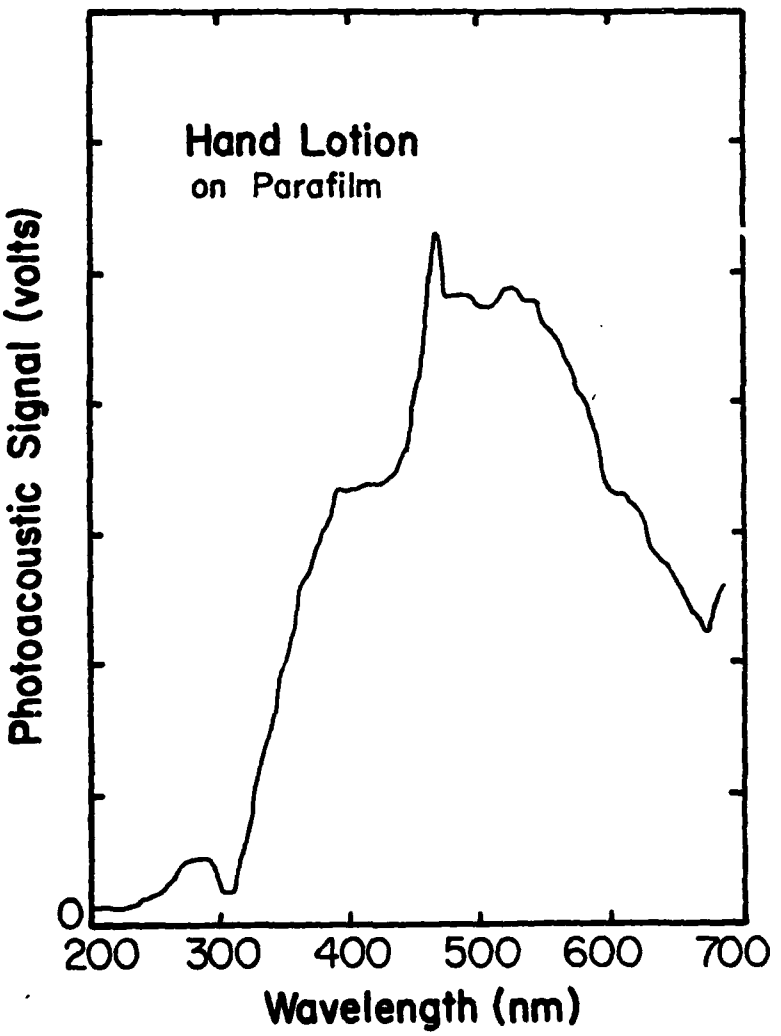

Figure 13. Smoothed Raw PAS Spectrum for a Film of a Commercial Hand Lotion on Parafilm.

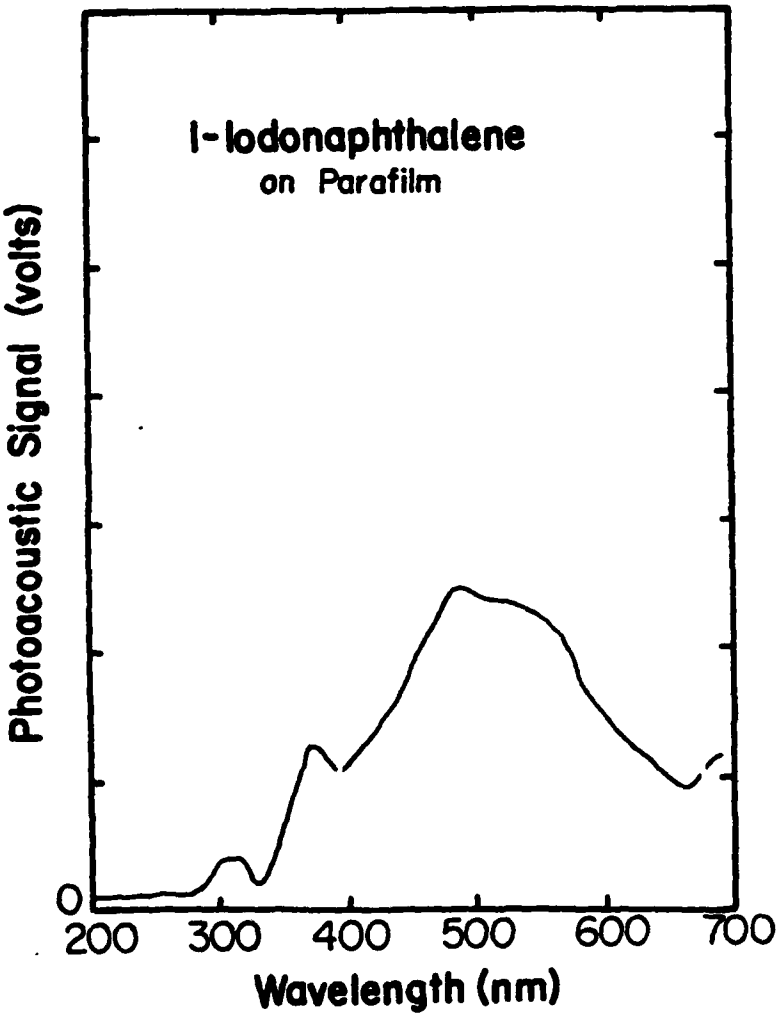

Figure 14. Smoothed Raw PAS Spectrum for a Film of the Hydrocarbon Fluid, 1-Iodonaphthalene, on Parafilm.

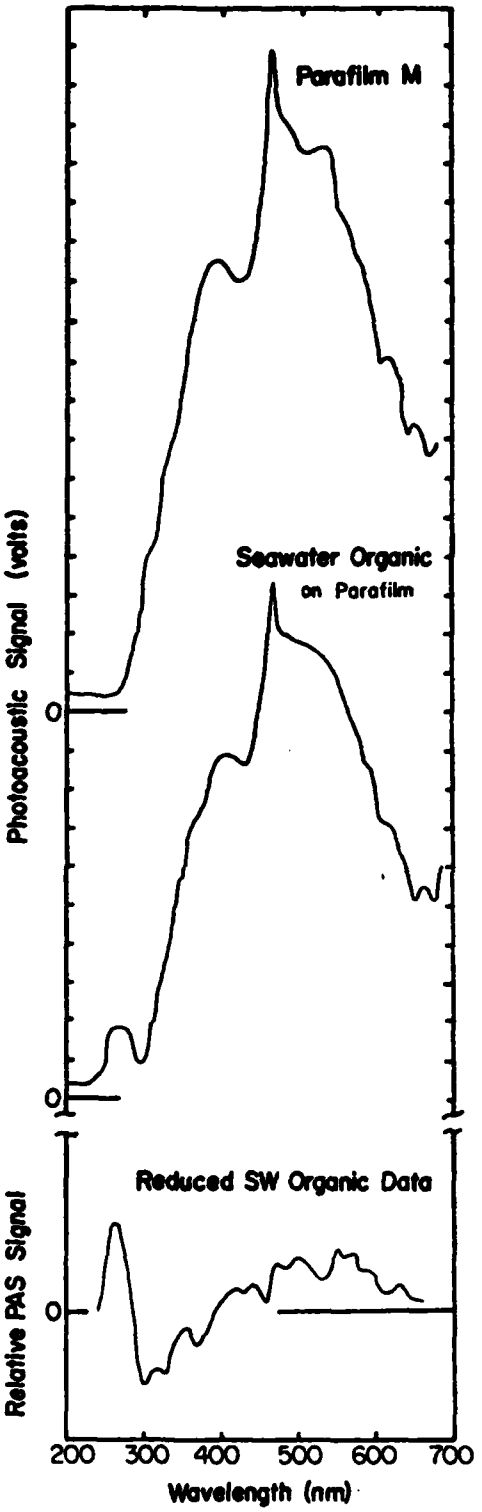

Figure 15. Smoothed Raw Spectra for Parafilm and for the Seawater Primary Film on Parafilm Shown above the Reduced Spectrum for the Seawater Primary Film Alone.

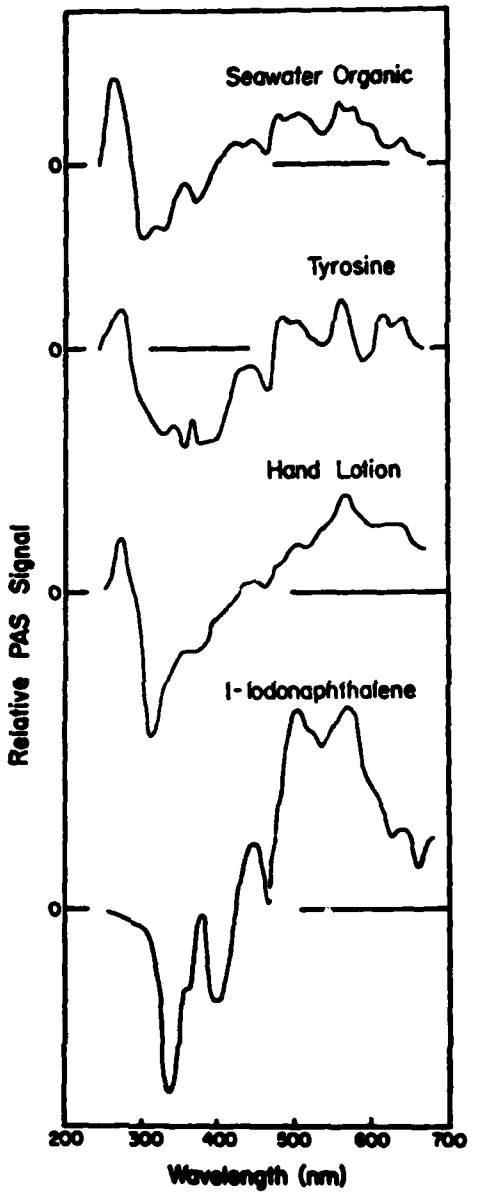

Figure 16. A Comparison of the Reduced PAS Spectra for the Four Organic Films Tested.

Figure Captions

Figure 1. Block Diagram of a typical photoacoustic spectrometer after Rosencwaig (1977).

Figure 2. Longitudinal cross-section of a single cylindrical photoacoustic cell showing the important cell dimensions.

Figure 3. Block diagram of a photoacoustic spectrometer using a water filled cell with hydrophone detector.

Figure 4. Photoacoustic spectrometer using a compound cell having water in the front chamber and air or some other gaseous fluid in the back chamber and a microphone detector.

Figure 5. Photoacoustic signal generation for the cell depicted in Figure 4. The sample thickness must be less than its thermal diffusion length.

Figure 6. Construction of the compound cell shown in Figure 4.

Figure 7. Mechanical, optical and electrical components of the photoacoustic spectrometer.

Figure 8. Raw PAS signal on carbon black representing the power spectrum of the Xenon arc lamp.

Figure 9. Raw PAS spectrum for a Parafilm sample.

Figure 10. Smoothed raw data for carbon black and Parafilm and the reduced Parafilm spectrum showing absorption bands centered at 370 and 530 nm.

Figure 11. Smoothed raw PAS spectrum for a four-day seawater primary film on Parafilm.

Figure 12. Smoothed raw PAS spectrum for the amino acid, Tyrosine, on Parafilm.

Figure 13. Smoothed raw PAS spectrum for a film of a commercial hand lotion on Parafilm.

Figure 14. Smoothed raw PAS spectrum for a film of the hydrocarbon fluid, 1-iodonaphthalene, on Parafilm.

Figure 15. Smoothed raw spectra for Parafilm and for the seawater primary film on Parafilm shown above the reduced spectrum for the seawater primary film alone.

Figure 16. A comparison of the reduced PAS spectra for the four organic films tested.

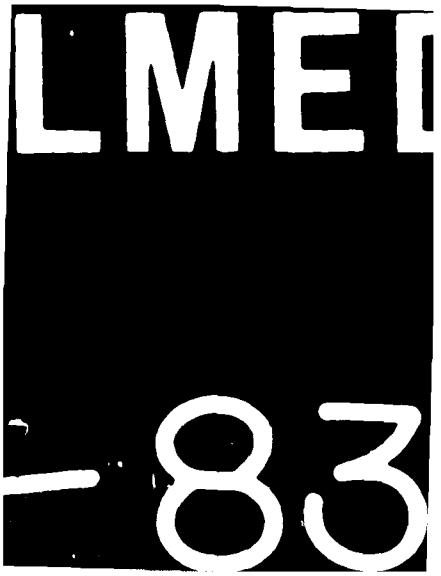
LMED
-83